Exploring the energy disposal immediately after bond-breaking in solution: the wavelength-dependent excited state dissociation pathways of *para*-methylthiophenol

Yuyuan Zhang,[1] Thomas A.A. Oliver,[2] Saptaparna Das,[1] Anirban Roy,[1] Michael N.R. Ashfold[2] and Stephen E. Bradforth[1*]

[1]*Department of Chemistry, University of Southern California, Los Angeles, CA 90089, USA*

[2]*School of Chemistry, Cantocks Close, University of Bristol, BS8 1TS, UK*

Fluorescence Experimental Methods

The static emission spectra were measured in a Fluoromax-3 spectrofluorometer (Horiba Scientific) with a 2 or 5 nm bandpass for excitation. Excitation centered at 266 nm was utilized throughout. The time-resolved emission was obtained by time-correlated single photo counting (TCSPC) (Becker and Hickl SPC-630, 22 ps time resolution) employing a 250 kHz regenerative amplified Ti:Sapphire laser system as source of femtosecond excitation pulses (Coherent RegA 9050). A portion of fundamental 800 nm was used to generate 532 nm from a two-stage optical parametric amplifier with type-I phase matching process (OPA 9450, Coherent). This OPA output was frequency-doubled to 267 nm, which was subsequently rotated to *s*-polarization (with purity better than 120:1), attenuated to < 1 nJ and focused to the sample by an f = 15 cm lens. The fluorescence of the *p*-MePhSH solution was collected at 90˚ to the excitation pulse. A calcite polarizer was set = 54.7˚ (magic angle) with respect to the 267 nm polarization to ensure isotropic detection along the fluorescence detection path. The wire-guided gravity jet was also used for the TCSPC experiments. The surface of the liquid jet was aligned to ~60° (instead of 45˚) to the excitation beam to avoid reflecting the excitation beam into the detector. Phenol

dissolved in cyclohexane solutions were used to optimize the angle and the position of the liquid jet, as phenol has a relatively high fluorescence quantum yield (~0.08)[1-4], well known fluorescence lifetime (2.1 ns in cyclohexane)[1,5,6] and low degradation yield at λ_{pump} = 267 nm. This unconventional sample delivery method for TCSPC was chosen because in both a static cell (with a stirrer bar), and a flow cell (with maximum linear flow rate of ~0.1 mm ms^{-1}) was found to degrade the p-MePhSH sample (see below) as observed by differences in UV absorption spectra acquired before and after laser exposure. With the wire-guided gravity jet, there was no change after a typical 20-minute scan.

10 mM p-MePhSH (97%, TCI America) and phenol (99.5%, Avocado) solutions were used in the TCSPC experiments with the wire-guided gravity jet (sample film thickness = 50–70 μm), whereas ~0.1 mM of solutions were used in other TCSPC experiments and all steady state emission measurements which utilized a 1 cm quartz static or flowing cell. The different concentrations for these two sets of experiments were used because the jet and cell have very different sample path lengths, but both required an optical density (OD) at 267 nm = ~0.1 to achieve satisfactory signal. Cyclohexane (> 99.99%, spectrophotometric grade, EMD), methanol (spectrophotometric grade, Macron Chemicals) and ethanol (200 proof, spectrophotometric grade, Sigma-Aldrich) were used as solvents without further purification. Most measurements were carried out in air. Steady-state fluorescence experiments in alcohol solvents were also carried out under rigorously nitrogen-purged conditions.

Steady State Emission Results – sensitivity to photoproducts

As noted in the main paper, we find that the photochemistry of p-MePhSH is so efficient that even under weak irradiation of the Xenon lamp of a fluorimeter with a 5 nm bandpass (centered at 266 nm), a minute or so irradiation rapidly leads to photoproduct buildup in a static fluorescence cuvette. For p-MePhSH dissolved in cyclohexane, initially there is no emission detectable above the small emission from impurities in the spectrophometric grade solvent. The photoproduct can then be detected by a newly developed fluorescence band between 300 – 320 nm or alternatively in the UV/visible absorption of the solution (Figs. S1(a-b)). Recording the UV/visible spectrum in the same fluorimeter cuvette as the UV exposure proceeds, we observe that absorption at 240 nm decreases whereas that at wavelength shorter than 230 nm increases (Fig. S1(c)), and the onset of the absorption spectrum develops a long wavelength tail (Fig. S1(c) inset). The latter can be used as a more general marker for determining if any permanent photoproduct is being produced by exposure to UV laser pulses.

When p-MePhSH is dissolved in alcohols, once again a buildup of a fluorescence band around 310 nm is observed that scales with 266 nm exposure time and inversely with flow rate of the solution through the exposure volume (data not shown). This exposure-dependent band is most similar to the one reported by Riyad *et al.*[7] Unlike in cyclohexane, different structured emission bands are observed immediately on placing the sample into the fluorimeter before the obvious onset of photochemistry. These appear at longer wavelength (340 – 410 nm), and are irreproducible from batch to batch of p-MePhSH, and depend methods of handling and solution preparation under nitrogen and de-aeration of the solution, or the choice of ethanol or methanol. (Methanol was also studied as it suffers from lower fluorescent impurities than ethanol). In all

cases these bands do not resemble a mirror image of the $S_1 \leftarrow S_0$ absorption and have too large a

Stokes shift to possibly originate from *p*-MePhSH. Additional evidence for this assignment to

impurities, in each case the fluorescence excitation spectrum does not have the same red onset as

for the *p*-MePhSH absorption spectrum. Given the absence of immediate emission in

cyclohexane, and irreproducible emission recorded in ethanol and methanol that appears to

depend on solution exposure to the smallest concentrations of oxygen, the balance of evidence

suggests that *p*-MePhSH has a vanishingly small quantum yield (see below) of S_1 emission.

Repeated failed attempts to record emission from the parent species suggests a variety of

impurities in the starting compound that are both air sensitive and are more soluble in alcohols

than in cyclohexane. However, even for solutions prepared in air, unlike the photo-products,

these impurities are present in such low concentration that they do not show up in the UV/Vis

absorption spectrum which is reproducible from experiment to experiment. They are only

observable because of the extreme sensitivity of fluorescence which amplifies a fluorescent

impurity (or photo-product) against a near-zero background from the primary solute and the

solvent.

We consider three possible candidates for the long-lived species accumulating by

photochemistry. MePhS radicals diffusively combine to dimerize to give MePhS-SPhMe (**1**), or

considering the alternate quinoidal resonance structure for MePhS, combination might lead to a
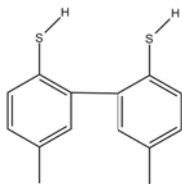
bi-thiophenol type structure (**2**) and finally 2-phenylsulfanylbenzenethiol (**3**)
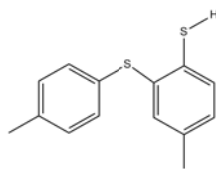
. We can check the absorption spectrum either from related compounds in the literature or from our own measurements of each against the spectrum seen growing in Fig. S1(c). Additionally, the photoproduct must have a reasonable fluorescence quantum yield. Kim *et al.* have identified the photoproduct of UV irradiation of substituted thiophenols in water/ethanol mixtures to be disulfides of the form (1).[8] Disulfides typically have long absorption tails to the red consistent with what is seen at $\lambda > 300$ nm in Figure S1. However, we have recorded the spectrum of commercially purchased *p*-tolyl disulfide (MePhS-S-PhMe) and attempts to reconstruct the series of absorption curves of Fig. S1(c) with increasing fractions of *p*-tolyl disulfide have been unsuccessful. Additionally, we have attempted to measured the fluorescence spectrum of purchased *p*-tolyl disulfide and found that the fluorescence yield of this molecule is small – close to solvent background levels and not enough to account for the drastic increase in fluorescence in the photoproduct contaminated *p*-MePhSH solution. Such a small fluorescence yield is in line with the ultrafast fission of the disulfide bond and generation of the *p*-MePhS radical as observed in TA experiment of *p*-tolyl disulfide.[9] Based on this evidence, we conclude that two photogenerated phenylthiyl radicals do not form the disulfide bond in the constant illumination photodegradation process.

Alternatively, radical combination might be expected to lead to a bi-thiophenol (or biphenyl dithiol) (**2**), similar to the bi-tyrosine or *o,o'*-bicresol identified in the photodegradation of tyrosine and *p*-cresol respectively.[10] *o,o'*-bicresol is characterized by a high quantum yield and emission at 310 nm and a broad band near 420 nm (the latter band is very similar to that we have observed from UV exposed *p*-MePhSH solutions in ethanol and methanol that have not been

rigorously excluded from air). The bi-tyrosine emission at 420 nm is well characterized and has

biphasic fluorescence decay (0.1-0.5 ns and ~ 4ns).[11] As *o,o'*-bi-thiophenol compounds are not

commercially available, we were unable to test their spectroscopic properties directly. The

synthesis and absorption spectrum of *p,p'*-biphenyldithiol derivative has been reported; the

UV/visible spectrum is in reasonable agreement with the regions where the absorption of the UV

exposed *p*-MePhSH grows with exposure time.[12] We have no information on the fluorescence of

biphenyldithiols, however, given the presence of the S–H moieties on each aromatic ring it

seems possible that the S_1 state would be predissociated in exactly the same way as *p*-MePhSH

and thus not fluorescent. But without information about the photochemistry of biphenyldithiols

we cannot rule out that compound (**2**) might be fluorescent and responsible for the photoproduct

emission.

Finally, thioethers are typically emissive.[13] MePhSMe has a long-lived singlet state at

room temperature [14] and diphenyl sulfide, PhSPh, which is most similar to (**3**) has fluorescent

emission at 320 nm and phosphorescence at 408 at 77K.[13] These are again similar wavelengths to

emission peaks detected here. PhSPh emission is however reported to be weak and with

nanosecond lifetime at room temperature.[15] Finally the absorption spectrum of PhSPh reported [15]

does not appear to have strong features where growth in the UV/visible of Figure S1(c) is

observed after irradiation.

Testing for photoproducts during course of femtosecond transient absorption experiments

The preceding discussion of the sensitivity of *p*-MePhSH to photo-degradation revealed by

attempts to reproduce the steady state fluorescence spectrum obviously raises concerns about the

integrity of a fresh sample used during a transient absorption experiment, which are the main results reported in this work. If photoproduct is generated under fluorimeter lamp conditions (0.35 mW at 267 nm with a bandpass of 5 nm) - to the extent that appreciable changes to the UV/vis spectrum are observable - it is reasonable to ask to what extent there is photoproduct buildup under laser intensity employed in the TA experiments (1.2 mW at 267 nm). The main difference in the two experiments is that the sample is under rapid laminar flow in the transient absorption experiments whereas it is either static or flowing very slowly in the steady state fluorescence. Even so, we carefully characterized the p-MePhSH solution using UV/Visible spectra in the same way as described in the previous section and found that solutions showed no difference after a typical 45-minute TA experiment (Fig. S1(d)). Similar results are obtained during TA experiments in ethanol solutions. This strongly suggests that the photoproduct does not build up to an appreciable extent. As described in Section II, the flow rate in the TA experiments (1 mm ms^{-1} achieved by the wire-guided gravity jet) and laser repetition rate ensures every laser pulse interrogating a fresh sample and thus eliminates the re-excitation problem. Therefore, we can conclude that transients probed in the pump/probe experiments are not contaminated by photoproducts. With respect to the much smaller amounts of oxidized impurity present in the purchased compound and revealed only in the alcohol emission spectra, we consider that as these are not observable in the UV/vis spectra, their contribution to the transient absorption experiments will be minor (less than 1% of any observed signal).

Fluorescence lifetimes by time-correlated single photon counting spectroscopy

To achieve comparable conditions for fluorescence characterization of p-MePhSH, we performed a fluorescence lifetime experiment using TCSPC also with the sample flowing in the

wire guided gravity jet apparatus. The linear flow rate minimizes the number of molecules being re-excited by subsequent laser pulses, but because of the laser higher repetition rate, the same sample volume still experiences ~10 laser pulses (the 266 nm spot size is smaller in TCSPC experiments than TA). Fig. S1(e) displayed the UV/Visible spectra before and after a typical 20-minute TCSPC experiment. Unlike the absorption spectrum after the experiment with a standard flow cuvette also tested (linear flow rate = 0.1 mm ms^{-1}), there is no significant difference between the original spectrum and that after 267 nm irradiation.

Once suitable flow conditions had been established such that no change is observed in the UV/visible spectrum before and after the experiments, we find that the integrated fluorescence counts from p-MePhSH in cyclohexane were reduced to less than 0.2% in comparison to our reference, phenol in cyclohexane (see Figure S2), and only just above the solvent background. Further, to record any emission counts at all from p-MePhSH, the laser intensity was increased by a factor of 20. This allows us to put an upper limit on the fluorescence quantum yield in cyclohexane, $\Phi_F = 10^{-5}$, a value considerably smaller than reported for any of the range of polar and non-polar solvents tested by Riyad et $al.$[7] This series of experiments carried out in our lab strongly suggests that the insufficient flow rate is the major reason for the build-up of the photoproduct and raises concerns over any experiment carried out without carefully taking the sample flow rate into consideration. Unlike the steady state experiments, the fluorescence lifetime experiments of Riyad et $al.$ used a 5 mm diameter flow cell, but no flow rate or laser spot size is specified in their paper, and a repetition rate of 10 Hz. It is unclear under conditions described by these authors whether a small amount of photochemical product is responsible for

the fluorescence lifetimes reported or whether there can still be a very small trapped sub-population left on S_1 particularly in polar solvents.

Ruling out 2PA contribution at early delay times supporting assignment for excited state radical

Examining the spectrum at $t = 0$ fs reveals a band centered right at 363 nm (Figure 2 and 8), near the expected absorption wavelength for the radical $\widetilde{D} \leftarrow \widetilde{A}$ transition. In the main paper, the connection is therefore made between the two to make the assignment of t = 0 fs signal to reaction product occurring within the ~ 50 fs instrument response. Let's take the opposite position here and argue that this $t = 0$ fs spectrum is in fact the coherent 2PA spectrum of p-MePhSH, arising from simultaneous absorption of one pump and one probe photon, and that there is no contribution at such early delay arising from a product induced by population created on the excited state surface by the pump pulse. (We note that the 2PA spectra of ethanol and cyclohexane[16,17] do not have peaks at this 2-photon energy – they rise monotonically, but quite steeply, towards short wavelength. However, we estimate that the non-resonant solvent 2PA only contributes at >5% of the total $t = 0$ signal shown in Figure 2 from 360 nm to *shorter* wavelengths, and at 320 nm is still no more than 20% of the signal)

We can test if the hypothesis of solute 2PA accounting for the signal is true by tuning the pump wavelength. For a coherent process, tuning the pump photon wavelength must change the absorbing wavelength of the probe, since the *total* 2PA energy (pump + probe) does not change for a given two-photon transition.[18] Specifically, if the λ_{probe} = 363 nm feature observed in λ_{pump} = 267 nm is indeed due to a transition to an unidentified higher excited state *via* 2PA, the transition energy would be 8.06 eV. Thus, tuning λ_{pump} to 295 nm would dramatically shift the probe absorption to a much shorter wavelength of 321 nm – see Fig. S3 for illustration. In light

of this, a ~40 nm blue shift of the peak in the probe absorption should be expected when the 295 nm pump is used. However, from examining the $t = 0$ fs spectra with three different pump wavelengths, it is apparent that there is no such shift when tuning the pump wavelength from 267 to 295 nm. Instead, the feature is always centered at 363 nm with λ_{pump} = 267, 285 and 295 nm (see Fig. S3). Therefore, the contribution of a coherent 2PA signal can be ruled out and this feature must originate from a transient species being produced within our instrument response time from pump-induced excited state population.

Adduct IR intensities

The vibrational waveumbers of each of the three adduct structures were calculated at the B3LYP/6-311+G* level in Gaussian03.[19] The results (shown in Table S1) were assessed for vibrations with large associated IR intensities with fundamental frequencies inside the 1400-1650 cm^{-1} window employed in UV-IR pump-probe studies.[20] The vibrational wavenumber calculations returned two sets of vibrations with associated large IR intensities for adduct A and B at 1532, 1538 and 1420 and 1418 cm^{-1}. These frequencies matched well with experimentally observed peaks (1520 and 1626 cm^{-1}) at a pump-probe time delay of 150 ps. One peak associated with adduct C was calculated to be 1639 cm^{-1}, matching excellently with the experimentally measured peak at 1625 cm^{-1}.

Decay Assisted Difference Spectra from target analysis

The kinetic model used in the target analysis of the main text is shown in Fig. S4(a). In this model, we treat each species → species dynamical transformation indicated by an arrow with a first order rate constant. Each species is described by a spectral basis function called a Decay Assisted Difference Spectra (DADS). We denote the initially excited state S^* realizing that at

270 nm excites an admixture of different states. The model is justified on the following physical grounds: Upon the excitation both $\tilde{A}$ and $\tilde{X}$ state radicals form very rapidly (compared to the experiment's ~50 fs instrument response) but a fraction of the molecules remained undissociated by trapping in the S_1 state. The $\tilde{A}$ state radical undergoes caging, which either leads to recrossing the S_2/S_0 CI to form $\tilde{X}$ state radical, or recombination on the diabat to the parent molecule (S_0). The trapped S_1 molecules will eventually dissociate to $\tilde{X}$ state radicals. The evolution of the population for each spectral component and the DADS obtained from the target analysis, are presented in Fig. S4(b) and (c), respectively. Fig. S4(c) also shows the calculated TDM^2 for the spectroscopic transitions for each species (as described in the main text). We note that fits (with very similar derived DADS) can be obtained with the same kinetic scheme from the 285 nm excitation dataset, taking into account the longer instrument response time.

As other kinetic connectivity schemes are certainly possible, we tried a number of variations. One other that yield good fits to the data while producing sensible DADS is shown in Figure S4(d-f). This can be considered a test for the robustness of the target analysis. Fig. 4S(e) and (f) reveals that DADS for each species are very similar to the previous model and the population evolution is similar in particular the $\tilde{X}/\tilde{A}$ branching probability is almost identical.

Fig. S5 presents the target analysis for the early delay time TA spectra obtained from 270 nm excitation of p-MePhSH in cyclohexane solution. The model employed in this case is identical to the one shown in Fig. S4(a), which yielded similar DADS for $\tilde{X}$ and $\tilde{A}$ radicals and the S_1 ESA. However, one significant difference from ethanol solution is immediately apparent. The $\tilde{A}$ state population is higher than $\tilde{X}$ state around $t = 0$ fs.

Table S1

Calculated harmonic and anharmonically corrected B3LYP/6-311+G* normal mode vibrational wavenumbers (cm^{-1}) and IR intensities (in km mol^{-1}) using Gaussian03 [19] for the three adduct molecules. Experimental results are from ref. 20.

Species	Calculated harmonic wavenumbers	Calculated anharmomic wavenumbers	Experimental wavenumbers	Calculated IR intensity
Radical	1610	1568	1575	113.50
Adduct A	1574	1532		94.96
			1520	
Adduct B	1579	1538		74.79
Adduct C	1678	1639	1625	103.30
Adduct A	1457	1420		43.91
			1425	
Adduct B	1448	1418		51.57

Figure S1 (next page)

(a) Fluorescence spectra of *p*-MePhSH in cyclohexane as a function of exposure (to UV light) time. The solutions were excited with 266 nm. The cyclohexane signal, which has a very weak fluorescent background and a large Raman response was subtracted. Note that the fresh sample (red line) has fluorescence counts close to zero. (b) overlay of the fluorescence spectrum of p-MePhSH in cyclohexane after exposed to UV for 5 minutes and that obtained by Riyad *et al*. (fluorescence spectrum of PhSH in 1-butyl chloride solution, re-plotted from Ref. [7]). (c) UV/Visible spectra of p-MePhSH in cyclohexane as a function of exposure time, obtained back-to-back with the corresponding trace shown in (a). Inset: the onset on the UV/Visible spectrum on an expanded scale. (d) UV/Visible spectra of *p*-MePhSH in cyclohexane obtained before and after a TA experiment. (e) UV/Visible spectra of p-MePhSH in cyclohexane obtained before and after TCSPC experiments. Blue line: obtained with a flow cell (linear flow rate = 0.1 mm ms^{-1}). Green line: obtained with a gravity-driven wire guided jet (linear flow rate = 1 mm ms^{-1}).
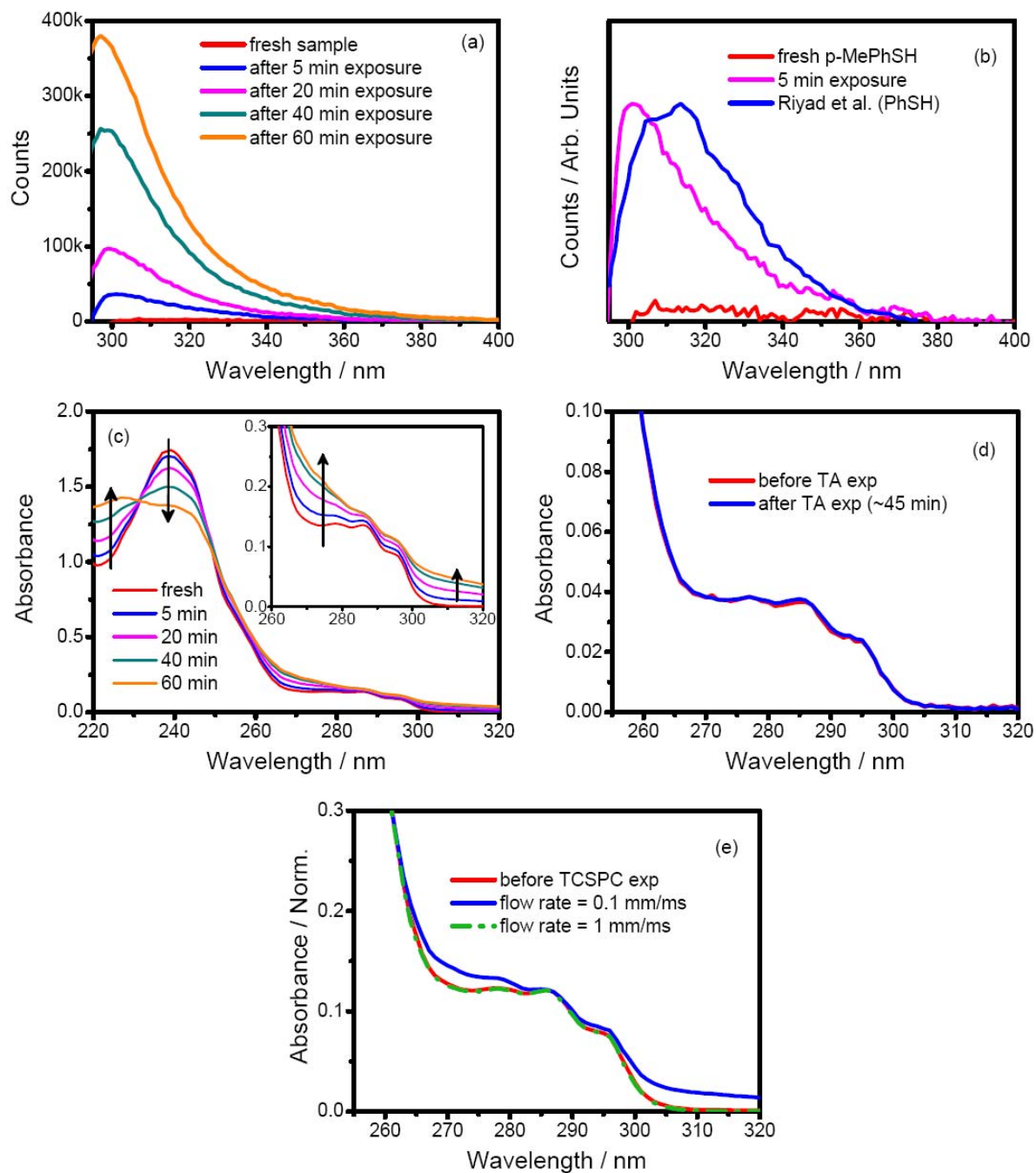
Figure S2

Fluorescence lifetime measurements of *p*-MePhSH compared to reference PhOH. Conditions are 10 mM phenol and *p*-MePhSH in cyclohexane; single pass of a solution through a gravity driven wire guided flow apparatus. Excitation is at 267 nm with 0.04 nJ (phenol) and 0.8 nJ (*p*-MePhSH) pulse energies at 250 kHz. Considering relative excitation energies, the literature quantum yield for PhOH ($\Phi_F = 0.075$)[4] and integration of photon counts under each curve yields an upper limit of $\Phi_F \sim 10^{-5}$ for *p*-MePhSH.
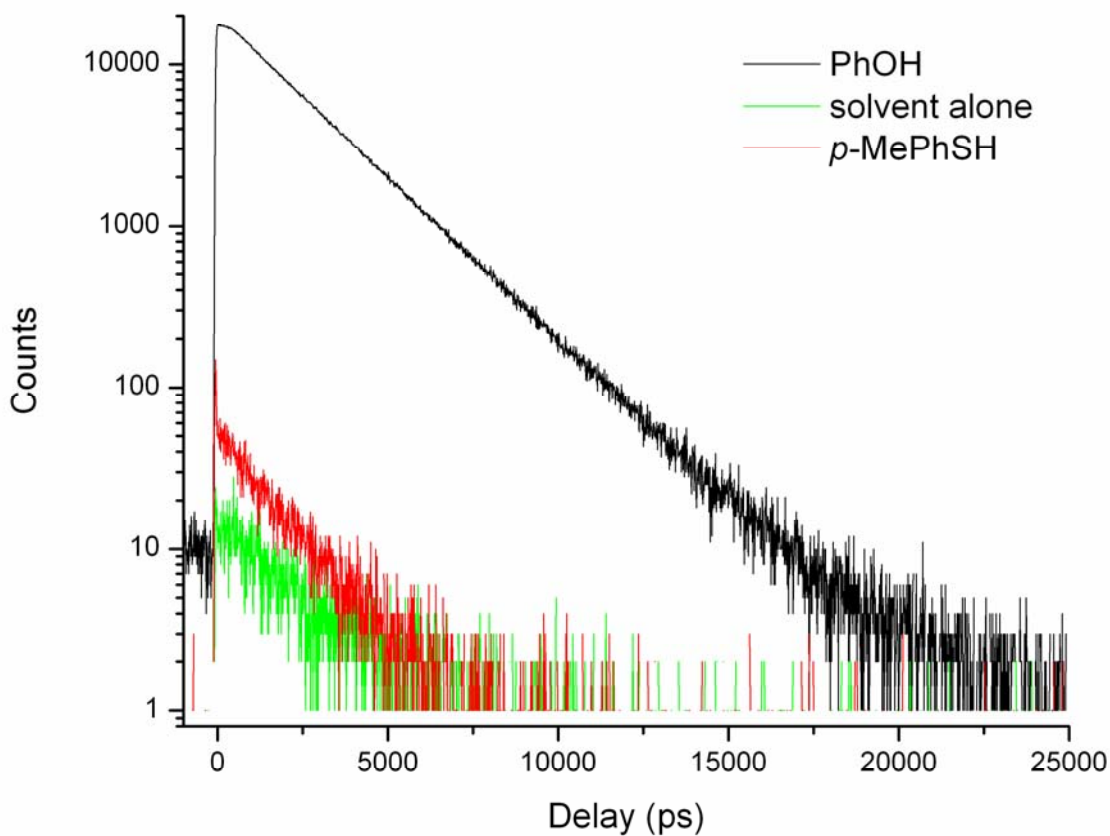
Figure S3

Left: Illustration of pump-probe combinations for a hypothetical 2-photon transition to an unidentified excited state (S_n), the transition energy is assumed to be 8.04 eV (calculated from the combination of 267 nm + 363 nm). **Right**: spectra at t = 0 fs for *p*-MePhSH in ethanol, excited with three different wavelengths. The ΔOD signals of the three traces were normalized at 363 nm. No such shifting 2PA peak is observed thus ruling out this hypothesis.
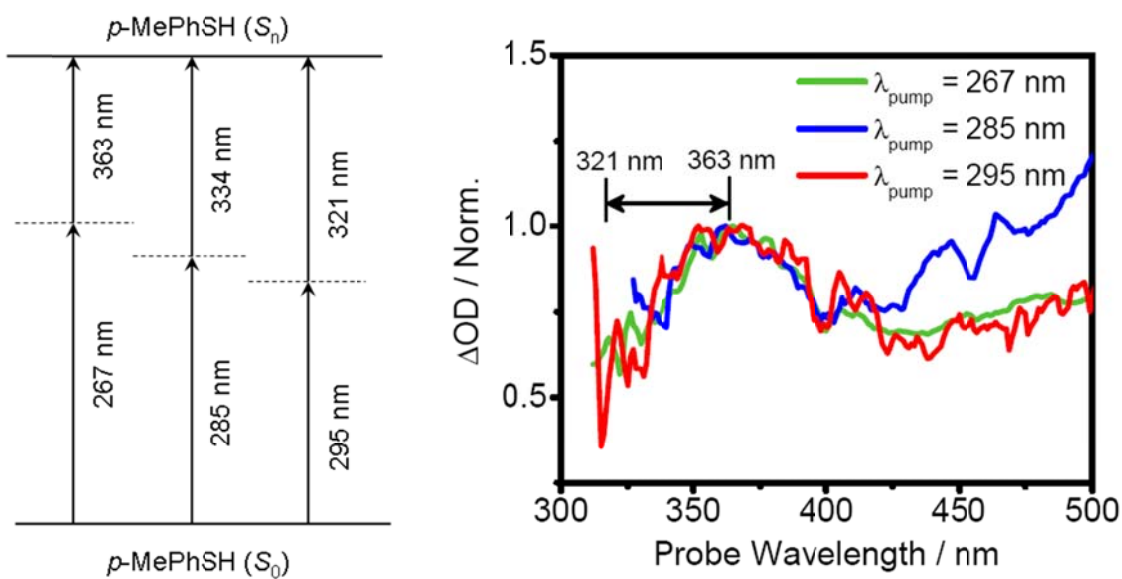
Figure S4

Results of global spectral fitting of 270 nm pump data in ethanol. (a) Kinetic model showing the species and their inter-connectivity, as well as best fit inverse rate constants, (b) species populations after convolution with instrument response function (c) and decay assisted difference spectra (c) for each transient species. The p-MePhS $\tilde{X}/\tilde{A}$ probability branching ratio determined by the respective rates out of S* is given by 0.016/0.021 = 0.8. This is the target model reported in the main text. (d – f): An alternative kinetic scheme is shown which yields a good fit and similar decay associated spectra - the p-MePhS $\tilde{X}/\tilde{A}$ probability branching ratio is similar (0.025/0.034 = 0.7).
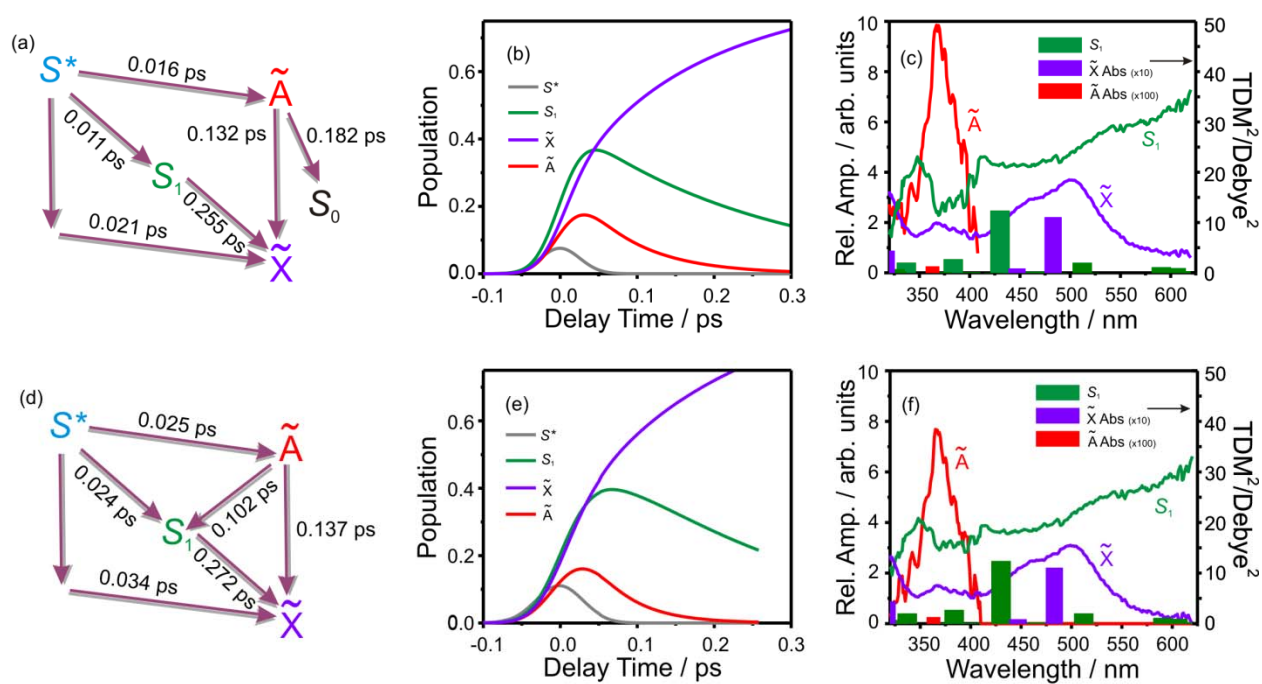
Figure S5

Results of global spectral fitting of 270 nm pump data in cyclohexane. (a) Kinetic model showing the species and their inter-connectivity (identical to Figure S4(a)), as well as best fit inverse rate constants, (b) species populations after convolution with instrument response function and (c) decay assisted difference spectra for each transient species. The p-MePhS $\tilde{X}/\tilde{A}$ probability branching ratio determined by the respective rates out of S* is given by 0.006/0.22 = 0.027.
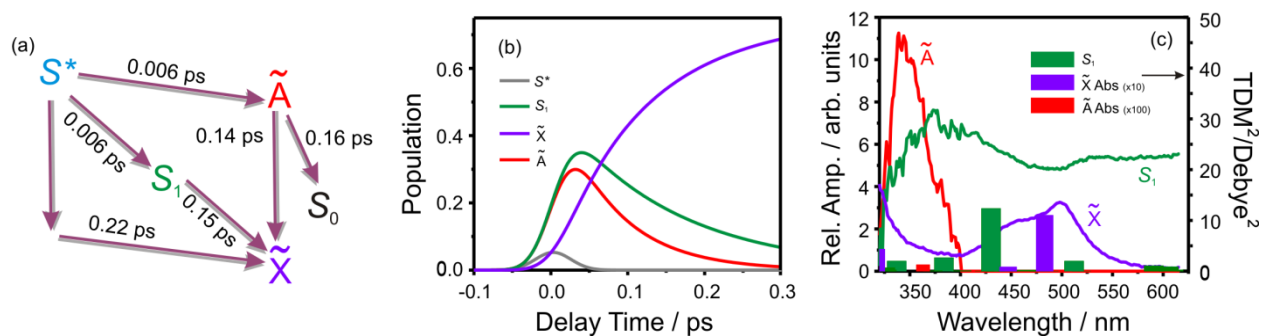
Figure S6

Comparison of anisotropies obtained by sequential and simultaneous measurements for 285 nm excitation of 90 mM *p*-MePhSH in ethanol solution. Sequential measurements are obtained by back-to-back experiments with the polarization of the pump and probe set to parallel and perpendicular. Simultaneous measurements are obtained by setting the polarization of the pump and probe to 45° and using a Wollaston prism to resolve the parallel and perpendicular component as described in the main text (See Experimental section). (a) Kinetics traces for 500 nm obtained at parallel and perpendicular polarization using the sequential method; (b) anisotropy calculated from traces shown in (a); (c) kinetics traces for 500 nm obtained at parallel and perpendicular polarization using the simultaneous method; (d) anisotropy calculated from trances shown in (c). The dash-dotted line indicates $R(t) = 0$.
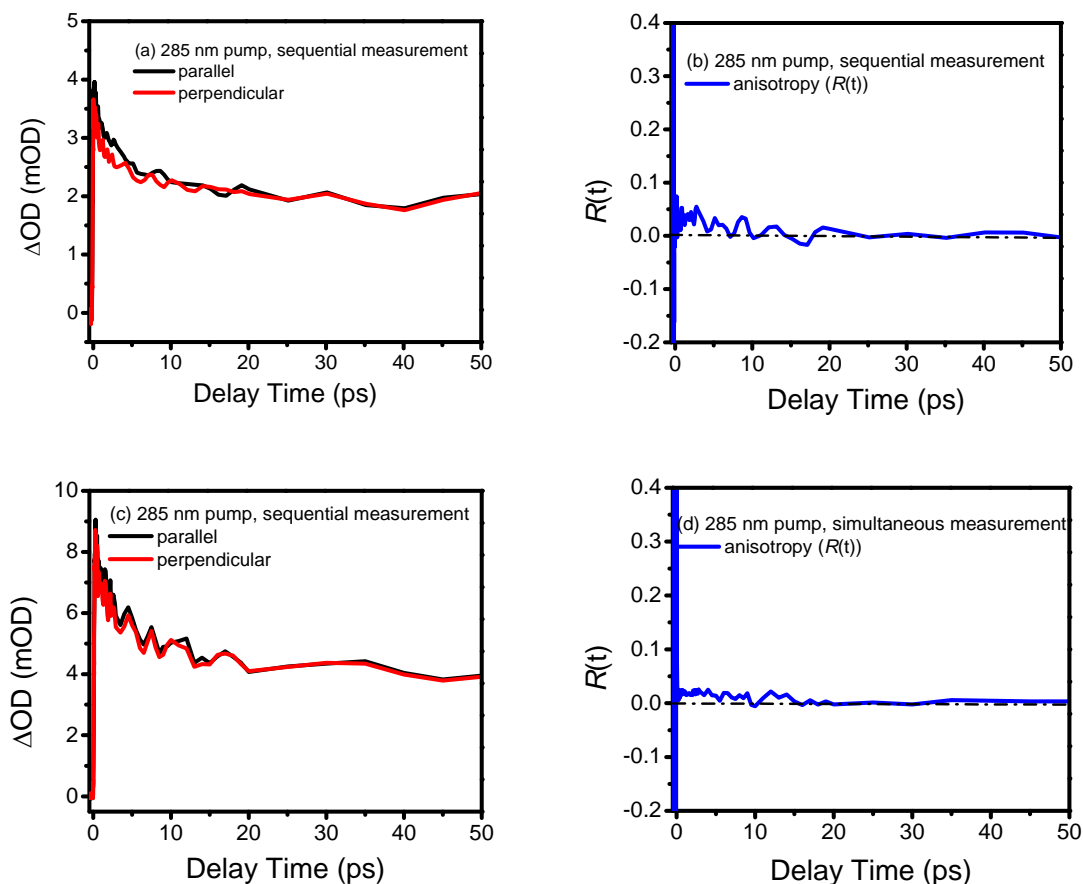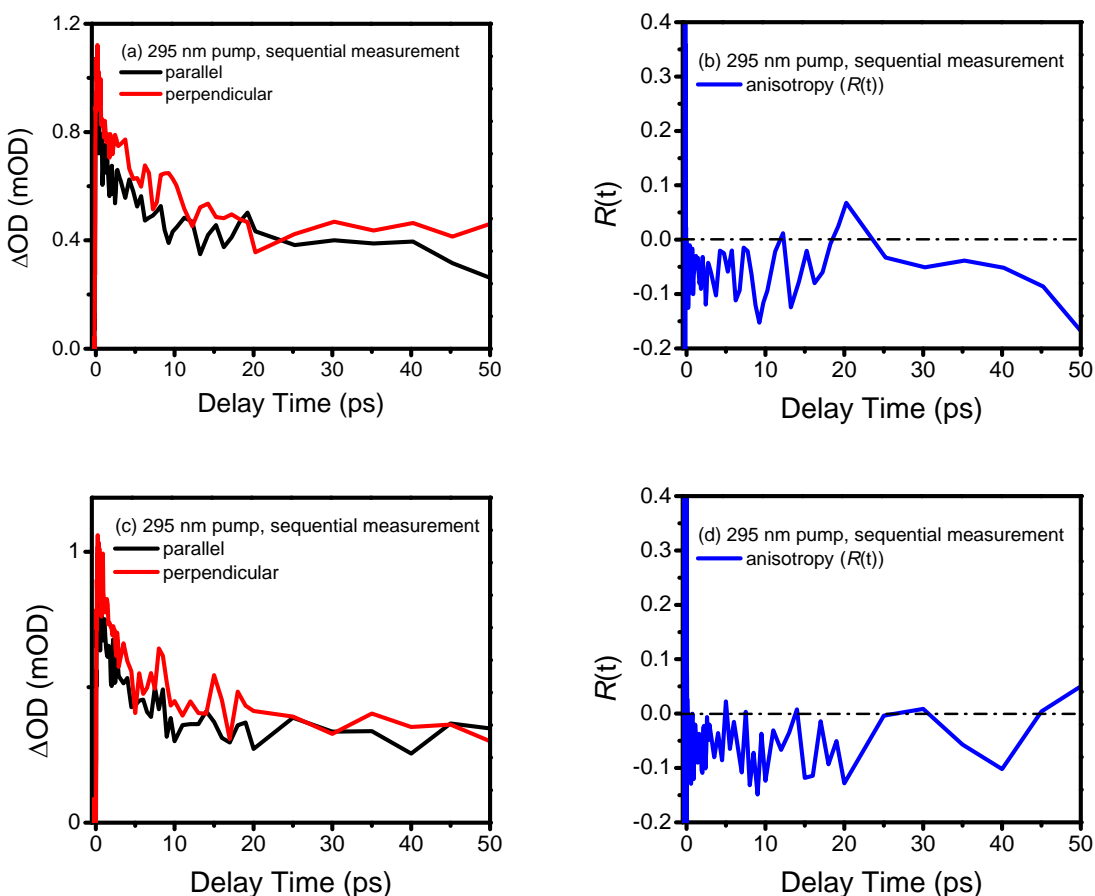
Figure S7

Comparison of anisotropies obtained by sequential and simultaneous measurements for 295 nm excitation of 90 mM *p*-MePhSH in ethanol solution. Sequential measurements are obtained by back-to-back experiments with the polarization of the pump and probe set to parallel and perpendicular. Simultaneous measurements are obtained by setting the polarization of the pump and probe to 45° and using a Wollaston prism to resolve the parallel and perpendicular component as described in the main text (See Experimental section). (a) kinetics traces for 500 nm obtained at parallel and perpendicular polarization using the sequential method; (b) anisotropy calculated from traces shown in (a); (c) kinetics traces for 500 nm obtained at parallel and perpendicular polarization using the simultaneous method; (d) anisotropy calculated from traces shown in (c). The dash-dotted line indicates $R(t) = 0$.

References for Supplemental Information:

1.   Berlman, I. B., *Handbook of Fluorescence Spectra of Aromatic Molecules*. Academic Press: New York, 1965.

2.   Kohler, G.; Getoff, N., Energy-Dependence and Solvent Effects in Deactivation of Phenol Molecules in Solution. *Chem. Phys. Lett.* **1974,** 26, 525-528.

3.   Kohler, G.; Getoff, N., Wavelength Dependence of Fluorescence Quantum Yield of Some Substituted Phenols. *J. Chem. Soc., Faraday Trans.* **1976,** 72, 2101-2107.

4.   Grabner, G.; Kohler, G.; Marconi, G.; Monti, S.; Venuti, E., Photophysical Properties of Methylated Phenols in Nonpolar-Solvents. *J. Phys. Chem.* **1990,** 94, 3609-3613.

5.   Sur, A.; Johnson, P. M., Radiationless Transitions in Gas-Phase Phenol and the Effects of Hydrogen-Bonding. *J. Chem. Phys.* **1986,** 84, 1206-1209.

6.   Lipert, R. J.; Bermudez, G.; Colson, S. D., Pathways of S1 Decay in Phenol, Indoles, and Water Complexes of Phenol and Indole in a Free Jet Expansion. *J. Phys. Chem.* **1988,** 92, 3801-3805.

7.   Riyad, Y. M.; Naumov, S.; Hermann, R.; Brede, O., Deactivation of the First Excited Singlet State of Thiophenols. *Phys. Chem. Chem. Phys.* **2006,** 8, 1697-1706.

8.   Kim, H. J.; Yoon, J. H.; Yoon, S., Photooxidative Coupling of Thiophenol Derivatives to Disulfides. *J. Phys. Chem. A* **2010,** 114, 12010-12015.

9.   Ashfold, M. N. R., *unpublished data*.

10.   Lehrer, S. S.; Fasman, G. D., Ultraviolet Irradiation Effects in Poly-L-Tyrosine and Model Compounds . Identification of Bityrosine as a Photoproduct. *Biochemistry* **1967,** 6, 757.

11.   Harms, G. S.; Pauls, S. W.; Hedstrom, J. F.; Johnson, C. K., *J. Fluorescence* **1997,** 7, 283-292.

12.   Shaporenko, A.; Elbing, M.; Baszczyk, A.; von Hanisch, C.; Mayor, M.; Zharnikov, M., Self-Assembled Monolayers from Biphenyldithiol Derivatives: Optimization of the Deprotection Procedure and Effect of the Molecular Conformation. *J. Phys. Chem. B* **2006,** 110, 4307-4317.

13.   Becker, R. S.; Jordan, A. D.; Kolc, J., Electronic Spectroscopy and Source of Spin-Orbit-Coupling in Phenyl Sulfides. *J. Chem. Phys.* **1973,** 59, 4024-4028.

14.   Harris, S. J.; Murdock, D.; Zhang, Y.; Oliver, T. A. A.; Grubb, M. P.; Orr-Ewing, A. J.; Greetham, G. M.; Clark, I. P.; Towrie, M.; Bradforth, S. E*., et al.*, Comparing Molecular Photofragmentation Dynamics in the Gas and Liquid Phases. *Phys. Chem. Chem. Phys.* **2013,** 15, 6567.

15.   Das, P. K.; Deslauriers, P. J.; Fahey, D. R.; Wood, F. K.; Cornforth, F. J., Photodegradation and Photostabilization of Poly(P-Phenylene Sulfide) .1. Laser Flash-Photolysis Studies of Model Compounds. *Macromolecules* **1993,** 26, 5024-5029.

16.   Zhang, Y.; Elles, C. G.; Rivera, C. A.; Oliver, T. A. A.; Bradforth, S. E., 2-Photon Absorption Spectroscopy of Alcohols and Alkanes. *in preperation*.

17.   Zhang, Y. Phd Thesis. University of Southern California, 2012.

18.   Elles, C. G.; Rivera, C. A.; Zhang, Y.; Pieniazek, P. A.; Bradforth, S. E., Electronic Structure of Liquid Water from Polarization-Dependent Two-Photon Absorption Spectroscopy. *J. Chem. Phys.* **2009,** 130, 084501.

19.   Frisch, M. J. T., G.W.; Schlegel, H.B.; Scuseria, G.E.; Robb, M.A.Cheeseman, J.R.; Montgomery Jr., J.A.; Vreven, T.; Kudin, K.N.; Burant, J.C.; Millam, J.M.; Iyengar, S.S.; Tomasi, J.; Barone, V.; Mennucci, B.; Cossi, M.; Scalmani, G.; Rega, N.; Petersson, G.A.; Nakatsuji, H.; Hada, M.; Ehara, M.; Toyota, K.; Fukuda, R.; Hasegawa, J.; Ishida, M.; Nakajima, T.; Honda, Y.; Kitao, O.; Nakai, H.; Klene, M.; Li, X.; Knox, J.E.; Hratchian, H.P.; Cross, J.B.; Adamo, C.; Jaramillo, J.; Gomperts, R.; Stratmann, R.E.; Yazyev, O.; Austin, A.J.; Cammi, R.; Pomelli, C.; Ochterski, J.W.; Ayala, P.Y.; Morokuma, K.; Voth, G.A.; Salvador, P.; Dannenberg, J.J.; Zakrzewski, V.G.; Dapprich, S.; Daniels, A.D.; Strain, M.C.; Farkas, O.; Malick, D.K.; Rabuck, A.D.; Raghavachari, K.; Foresman, J.B.; Ortiz, J.V.; Cui, Q.; Baboul, A.G.; Clifford, S.; Cioslowski, J.; Stefanov, B.B.; Liu, G.; Liashenko, A.; Piskorz, P.; Komaromi, I.; Martin, R.L.; Fox, D.J.; Keith, T.; Al-Laham, M.A.; Peng, C.Y.; Nanayakkara, A.; Challacombe, M.; Gill, P.M.W.; Johnson, B.; Chen, W.; Wong, M.W.; Gonzalez, C.; Pople, J.A. *Gaussian 03*, Revision B.04; Gaussian Inc., Pittsburgh PA.: 2003.

20.   Murdock, D.; Harris, S. J.; Karsili, T. N. V.; Greetham, G. M.; Clark, I. P.; Towrie, M.; Orr-Ewing, A. J.; Ashfold, M. N. R., Photofragmentation Dynamics in Solution Probed by Transient Ir Absorption Spectroscopy: Pi Sigma*-Mediated Bond Cleavage in P-Methylthiophenol and P-Methylthioanisole. *J. Phys. Chem. Lett.* **2012,** 3, 3715-3720.